

# Predicting Effectiveness of H<sub>2</sub>O Injection for NO<sub>x</sub> Reduction in Stationary Gas Turbines

A. M. Mellor\*

*Vanderbilt University, Nashville, Tennessee 37235-1592*

Water or steam injection in stationary gas turbines with conventional combustors is a well-established technique for NO<sub>x</sub> emissions control, but development programs to establish the best inert insertion method are time consuming and expensive. A model previously calibrated with fielded, heavy-duty combustion turbines is applied here to an industrial gas turbine, and the resulting quite accurate predictions of NO<sub>x</sub> reduction confirm that an optimum configuration has also been selected for the latter. Lowering of stoichiometric flame temperature by evaporation and dilution is the governing process considered in the model. However, this model fails to account for the nitrous oxide route to NO formation and does not explain a measured trend that inert injection becomes slightly more effective as engine power output is increased. Thus, a second model including both Zeldovich and nitrous oxide pathways is introduced. When the calibration and prediction processes are repeated for the three engines considered, an explanation for the second-order effect on NO<sub>x</sub> reduction is suggested: kinetic, flame-front O-atom overshoot vs equilibrium decreases with increasing engine load, so that less NO formation occurs via the nitrous oxide route as combustion pressure rises.

## Nomenclature

$a$	=	molar ratio of water-to-fuel flow rate
$K_{c6}$	=	equilibrium constant based on concentrations for $O_2 \rightleftharpoons 2O$ , reaction (6)
$k$	=	specific reaction rate coefficient, $cm^3/gmol \cdot s$ if bimolecular
$M$	=	third body in termolecular reaction
NO <sub>x</sub>	=	oxides of nitrogen, NO and NO <sub>2</sub>
NO <sub>x</sub> EI	=	oxides of nitrogen emissions index, g NO <sub>x</sub> as NO <sub>2</sub> /kg fuel
$p$	=	combustor inlet pressure, atm
$R$	=	universal gas constant, $82.06 \text{ atm} \cdot \text{cm}^3/\text{gmol} \cdot \text{K}$
$r$	=	correlation coefficient
$T$	=	temperature, K
$T_{\phi=1}$	=	adiabatic stoichiometric flame temperature, K
$x$	=	equilibrium mole fraction
$\sigma$	=	standard deviation of the $y$ values for the observed values of $x$
$\tau_{no}$	=	characteristic kinetic time for NO formation, s
$\phi$	=	fuel–air equivalence ratio

## Subscripts

all	=	all inert going to the stoichiometric eddies
dry	=	no inert injection
H <sub>2</sub> O	=	water or steam injected
no	=	nitric oxide
$s$	=	static
wet	=	with inert injection
0	=	low-pressure limit
0.1 ms	=	value at 0.1 ms residence time
1 $f$	=	$O + N_2 \rightarrow NO + N$ , reaction 1 $f$
3	=	combustor inlet
5 $f$	=	$O + N_2 + M \rightarrow N_2O + M$ , reaction 5 $f$
100 ms	=	value at 100 ms residence time
$\infty$	=	high-pressure limit

## Introduction

SOME purchasers of aeroderivative and heavy-duty gas turbines for power generation prefer water or steam injection in conventional combustors to dry, low-emissions designs for NO<sub>x</sub> reduction. The rationale is based on the concern that combustion pressure oscillations, auto-ignition, or flashback will lead to more frequent plant outages with the newer technology. As a result, equipment manufacturers must test different water/steam injectors and positions in each combustor offered for this market. Frequently, the optimal design is established only by brute force, a process that is expensive. Models that can be used to predict the optimum are, thus, cost-effective.

Touchton<sup>1</sup> compared natural-gas-fired results in the literature and from his own extensive test series with perfectly stirred reactor calculations for stoichiometric combustion of methane with air/steam mixtures. Zeldovich chemistry was employed to model NO formation in burned gases otherwise at equilibrium. In general, he found measured NO<sub>x</sub> reductions were less than theoretical and demonstrated that neither mixing of steam with fuel nor, for water injection in place of steam, evaporation was responsible for the discrepancy between measurement and calculation.

More recent inert injection modeling efforts include both computational fluid dynamics<sup>2</sup> (CFD) and semi-empirical approaches.<sup>3</sup> This work is concerned with the latter, because results from the CFD analysis were consistently too low when compared with measurements,<sup>2</sup> possibly due to overprediction of temperature reductions. The technique developed previously<sup>3</sup> with 150-MW combustion turbines is applied here to the same 3.25-MW industrial gas turbine, the AlliedSignal ASE40, examined by Liever et al.<sup>2</sup> It is also based on the reduction in stoichiometric flame temperature associated with inert injection slowing the extended Zeldovich mechanism thought responsible for thermal NO formation in a conventional combustor.

Effectiveness of water or steam injection is defined as the reduction in emissions actually obtained compared with the theoretical maximum.<sup>1,3</sup> In the previous work with the combustion turbines, a 70% effectiveness was observed<sup>3</sup> from the correlation of the data. In the present study it is shown that this value also predicts the results with the industrial turbine quite accurately. However, a systematic but second-order trend, also reported by Touchton<sup>1</sup> and Toof,<sup>4</sup> is encountered: At a given water-to-fuel ratio, the reduction in NO<sub>x</sub> emissions increases slightly as load (combustor inlet air temperature, pressure, air flow rate, and overall equivalence ratio) is increased.

Toof<sup>4</sup> modeled NO formation from the prompt, fuel–nitrogen, and Zeldovich mechanisms and suggested that the first may

Received 12 April 1999; revision received 28 August 1999; accepted for publication 3 September 1999. Copyright © 1999 by A. M. Mellor. Published by the American Institute of Aeronautics and Astronautics, Inc., with permission.

\*Centennial Professor, Box 1592, Station B, Mechanical Engineering, Associate Fellow AIAA.

contribute to a leveling off of  $\text{NO}_x$  reductions if water-to-fuel ratio by mass exceeds unity. However, he did not evaluate the  $\text{N}_2\text{O}$  mechanism,<sup>5</sup> now known to be important to  $\text{NO}$  formation in diluted flames (i.e., flame temperatures lower than stoichiometric) at elevated pressures.<sup>6</sup> It is possible that  $\text{N}_2\text{O}$  chemistry is responsible for the observation noted that improved effectiveness is obtained as load is increased. Therefore, a second semi-empirical approach, based on both Zeldovich and nitrous oxide chemistry, is also presented, calibrated with the heavy-duty data, and then applied to predict the data from the industrial combustor. This new model for  $\text{NO}_x$  reduction by inert injection in gas turbines is the first to include the  $\text{N}_2\text{O}$  mechanism.

## Results

### Nature, Ranges, and Quality of Data

The data analyzed here (24 total) were supplied by AlliedSignal and do not correspond directly to those reported previously.<sup>2</sup> The combustor in the ASE40 engine is annular with reverse airflow from the compressor. The design is conventional, with 28 integral fuel/water injectors, each mounted in an axial air swirler on the combustor dome. Cross-sectional views of the engine hot section and natural gas/water injector are shown in Figs. 1 and 2, respectively. Engine load is indexed from idle to 4200 (full load), and liquid water injection sweeps at a given load such as, for example, 2025, which is approximately a half load with a water-to-fuel mass ratio of 0.3348. The load designation ( $x \times 00$ ) gives nominal engine output in horsepower, where the last two digits represent relative water-to-fuel ratios ( $x \times 00$  is dry). Maximum water-to-fuel ratio by mass used in these engine tests is 1.08. Combustor air inlet temperatures  $T_3$  and pressures  $p_{s3}$  increase from 509 K, 4.22 atm at idle to 633 K, 8.29 atm at the most severe operating condition tested (4375).

All tests considered hereafter were conducted with natural gas fuel ( $\text{H/C} = 3.88$ ) modeled here as  $\text{CH}_4$  for the requisite flame-temperature calculations. Fuel flow is increased as water is increased to maintain approximately constant engine power output. The range of overall equivalence ratios  $\phi$  represented in the data is 0.198–0.355.

Standard averaging probes and instrumentation were employed to obtain engine exhaust values of  $\text{O}_2$ ,  $\text{CO}_2$ ,  $\text{CO}$ ,  $\text{HC}$  (as  $\text{CH}_4$ ), and total oxides of nitrogen ( $\text{NO}_x$ ). Measured combustion efficiencies exceed 99%, with all but four values greater than 99.6%. The ratio of oxygen

in the exhaust calculated from the emissions to that measured in the gas samples averages 0.9981 with 0.9959 being the minimum and 1.0021 being the maximum.

### Prediction of the Data

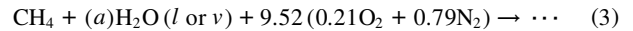
Newbury and Mellor<sup>3</sup> have demonstrated the correlation of  $\text{NO}_x$  emissions index ( $\text{NO}_x \text{EI}$ ) reduction for both gas- and oil-fired 150-MW combustion turbines using the following relation that they derive in full:

$$\text{NO}_x \text{EI Reduction} \equiv \frac{\text{NO}_x \text{EI}|_{\text{wet}}}{\text{NO}_x \text{EI}|_{\text{dry}}} = \frac{T_{\phi=1,\text{dry}}}{T_{\phi=1,\text{H}_2\text{O}}} \exp \left[ 67,975.83 \left( \frac{1}{T_{\phi=1,\text{dry}}} - \frac{1}{T_{\phi=1,\text{H}_2\text{O}}} \right) \right] \quad (1)$$

where the apparent activation temperature within the exponential term is in degree Kelvin. This expression is valid ignoring the small changes in total combustor flow rate and burned gas molecular weight as water-to-fuel ratio is increased. In Eq. (1), dry mole fraction units at 15%  $\text{O}_2$  gas content (parts per million by volume dry at 15%  $\text{O}_2$ ) can be substituted for EI with essentially identical results for the data correlated here, and the stoichiometric flame temperature with inert injection that correlated the data via Eq. (1) is

$$T_{\phi=1,\text{H}_2\text{O}} = 0.7T_{\phi=1,\text{all}} + 0.3T_{\phi=1,\text{dry}} \quad (2)$$

In the case of gas firing, both temperatures on the right-hand side of Eq. (2) were computed with STANJAN<sup>7</sup> via



Here ( $a$ ) is the molar water (for the ASE40 tests liquid  $l$ ) to fuel ratio used to compute  $T_{\phi=1,\text{all}}$  (all water to stoichiometric eddies<sup>3</sup>) and equals zero for the  $T_{\phi=1,\text{dry}}$  calculation. For each ASE40 load and water-to-fuel datum, the fuel and inert were assumed at 298 K, the air at its inlet temperature  $T_3$ , and the pressure was taken constant at  $p_{s3}$ .

Results of the model predictions are shown in Fig. 3. Here the measured  $\text{NO}_x \text{EI}$  reductions are graphed vs the  $\text{NO}_x \text{EI}$  reductions predicted from Eqs. (1–3). All dry data, irrespective of power level, appear at the coordinates (1,1) by definition, and so the water-to-fuel ratio is increased at a given power level from this position to the

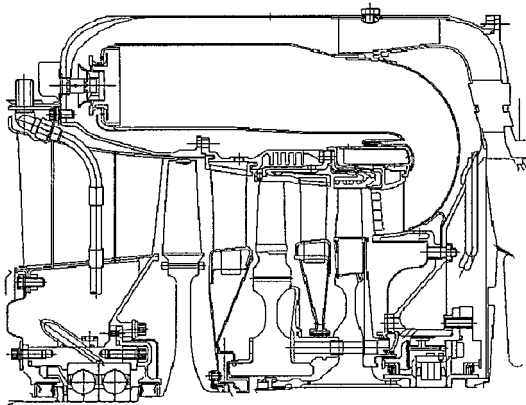


Fig. 1 ASE40 hot section cross section.<sup>2</sup>

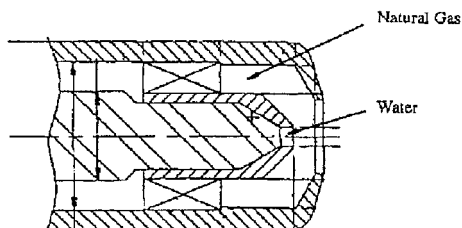


Fig. 2 Natural gas/water injection nozzle cross section.<sup>2</sup>

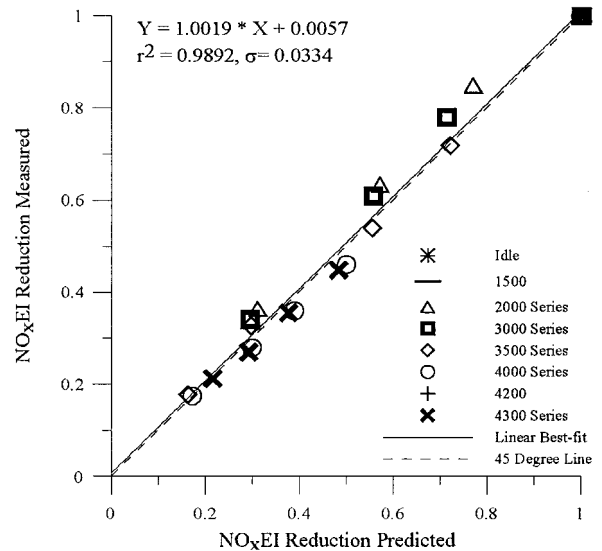


Fig. 3 Measured vs predicted  $\text{NO}_x$  reductions for the AlliedSignal ASE40 industrial gas turbine operating over its load range either dry or with liquid water injection [the predictions are based on the method of Newbury and Mellor<sup>3</sup> that accounts for the lowering of stoichiometric flame temperature by water evaporation/dilution, with 70% effectiveness, see Eq. (2), and corresponding decrease in  $\text{NO}$  formation rate via the Zeldovich mechanism].

origin. The dashed line at 45 deg indicates the result expected for a perfect prediction of the measured values. A least-squares fit of the results is shown as the solid line, and its equation, squared correlation coefficient, and standard deviation are shown in the legend.

Although all 24 data are included in Fig. 3, water-to-fuel variations were not reported by AlliedSignal for either the 1500 datum near engine idle or the 4200 datum at full load. Furthermore, no dry measurement was available for the 4300 point, and so it was estimated as 6.95 g/kg from Eq. (1) using the dry stoichiometric flame temperatures and the dry 4200 measurement.

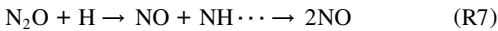
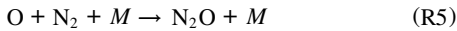
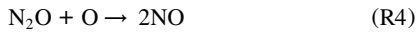
From Fig. 3 it is seen that the model has captured the primary effect of water injection on emitted nitrogen oxides, which is the lowering of adiabatic stoichiometric flame temperature and the consequent decreasing of thermal NO formation rate.<sup>1,3,4</sup> Reductions greater than 80% from the dry value are observed in both the 3500 and 4000 series at the maximum water-to-fuel ratios tested. The predictions are quite accurate, as indicated by the high correlation coefficient, low standard deviation, fit slope very near unity, and  $y$  intercept near zero. However, the second-order effect found by Touchton<sup>1</sup> and Toof<sup>4</sup> is also shown clearly in Fig. 3: The lower load 2000 and 3000 series data fall above the fit equation, whereas the remaining higher load measurements are below the solid line at intermediate values of water-to-fuel ratio. Note that the only load-dependent terms in Eqs. (1–3) are the various values of dry and diluted stoichiometric flame temperature, which increase with  $T_3$  and slightly as  $p_{s3}$  is increased due to the resulting suppression of dissociation.

#### Inclusion of Nitrous Oxide Chemistry

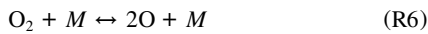
For flames diluted with air or inert, Malte and Pratt<sup>5</sup> have established that  $N_2O$  chemistry participates in NO formation (see, for example, Refs. 5 and 6). Briefly, the recommended<sup>6,8</sup> skeletal mechanism for NO formation consists of the three reactions of the extended Zeldovich mechanism:



and three reactions responsible for NO formation via the  $N_2O$  mechanism,



where the missing reaction (R6) represents the commonly assumed O-atom in equilibrium with  $O_2$ ,



The controlling rate coefficients are shown in Fig. 4 in Arrhenius format for both the Zeldovich ( $k_{1f}$ ) and  $N_2O$  or third-body ( $k_{5f}$ ) mechanisms, the dark and light solid lines, respectively, as functions of diluted stoichiometric flame temperature and combustor pressure.<sup>9</sup> The specific reaction rate coefficient for the nitrous oxide route is fuel and pressure dependent, as shown in Fig. 4, so that at higher pressures and lower temperatures the third-body reaction (5)  $O + N_2 + M$  becomes competitive with the lead reaction (1)  $O + N_2$  in the Zeldovich chemistry. To obtain Fig. 4, both N-atom and  $N_2O$  are assumed in steady state, and third-body collision efficiency, evaluated per the methane Gas Research Institute (GRI) mechanism 2.11 following the recommendations of Bowman et al.,<sup>10</sup> is computed for chemical equilibrium at the flame conditions.<sup>9</sup> Details are provided hereafter.

For the range of natural-gas-fired ASE40 data considered here, combustor pressures fall between 4.22 and 8.29 atm, as noted earlier, and reciprocals of computed stoichiometric flame temperatures

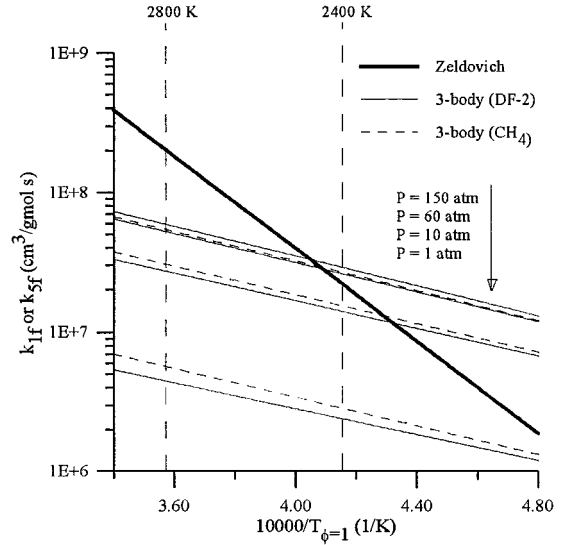


**Fig. 4** Contribution of the Zeldovich and  $N_2O$  mechanisms to the NO formation rate in Arrhenius format for various engine conditions; logarithms are presented as functions of inverse stoichiometric flame temperature in the approximate range from 2100 to 2900 K, so that midrange values correspond to dry stoichiometric values, with pressure as a parameter.<sup>9</sup>

vary from  $4.12 \times 10^{-4}$  to  $4.55 \times 10^{-4} \text{ K}^{-1}$ . Examination of Fig. 4 indicates that the contribution of the nitrous oxide mechanism to ASE40 wet oxides of nitrogen emissions is important for this range of burned gas conditions. Furthermore, because the relative contribution of the specific reaction rate coefficients has a different dependence on both flame temperature and pressure, and thus engine load, than the model developed previously,<sup>3</sup> it is possible that the effectiveness of water injection as a function of load can be explained based purely on the chemical kinetics. Accordingly, a new model including both Zeldovich and nitrous oxide chemistry is introduced.

The equation for conventional combustors that replaces Eq. (1) is

$$\frac{NO_x EI|_{\text{wet}}}{NO_x EI|_{\text{dry}}} = \frac{T_{\phi=1, \text{dry}}}{T_{\phi=1, H_2O}} \frac{\tau_{no, \text{dry}}}{\tau_{no, H_2O}} \frac{x_{no, H_2O}}{x_{no, \text{dry}}} \quad (4)$$

where  $\tau_{no}$  is a characteristic time for NO formation and  $x_{no}$  is the equilibrium NO mole fraction in the burned gas. Mello and Mellor<sup>11</sup> derive the emissions index expression for lean premixed gas turbine combustors including Zeldovich and nitrous oxide mechanisms.

Assuming the O-atom and  $N_2$  are in equilibrium in the burned gas as well, then the characteristic time is evaluated as<sup>12</sup>

$$\tau_{no} = \frac{[NO]}{2[O][N_2](k_{1f} + k_{5f})} \quad (5)$$

where brackets indicate equilibrium concentrations. From Bowman et al.,<sup>10</sup>

$$k_{1f} = 1.63 \times 10^{14} \exp(-38095/T_{\phi=1}) \quad (6)$$

whereas for recombination reactions<sup>13</sup>

$$k_{5f} = k_{5f, \infty} / \left( 1 + \frac{k_{5f, \infty}}{k_{5f, 0}[M]} \right) \quad (7)$$

In Eq. (7) the effective third-body concentration for the range of ASE40 operation is computed from the equilibrium burned gas compositions as

$$[M] = (p_{s3}/RT_{\phi=1, \text{all}})(0.3669a + 2.0107) \quad (8)$$

where  $R$  is the universal gas constant, and<sup>10</sup>

$$k_{5f, \infty} = 5.45 \times 10^9 \exp(-12430/T_{\phi=1}) \quad (9)$$

$$k_{5f, 0} = 2.6 \times 10^{13} \exp(-10672/T_{\phi=1}) \quad (10)$$

Preexponential factors in Eqs. (6), (9), and (10) are expressed in gram mole, cubic centimeters, and seconds, and, as in Eq. (1), the activation temperatures are in degrees Kelvin. Further details of the nitrous oxide chemistry can be found in Refs. 12 and 14. Either the dry or effective stoichiometric flame temperature [defined hereafter, but similar to that in Eq. (2)] is substituted for  $T_{\phi=1}$  in the preceding equations, according to Eq. (4).

There are two ways in which to evaluate this model including both Zeldovich and nitrous oxide kinetics. The first is to use the ASE40 data and determine the effectiveness as a function of engine load through the model represented by Eqs. (4–10). However, the result of applying this method is a correlation, not a prediction. Consequently, instead the combustion turbine correlation of Newbury and Mellor<sup>3</sup> is reestablished with the new model. For these higher pressure (modeled here as 13 atm) and somewhat wider flame temperature ranges (2203–2445 K), the effective third-body concentration given by Eq. (8) compares to within 0.6% or better of the value computed directly at the appropriate equilibrium conditions.

This procedure results in a new effectiveness of water injection of 62.8% for the combustion turbines; that is, to apply the new model to reproduce the combustion turbine data

$$T_{\phi=1, \text{H}_2\text{O}} = 0.628T_{\phi=1, \text{all}} + 0.372T_{\phi=1, \text{dry}} \quad (11)$$

This lower effectiveness, when accounting for formation of NO through both the Zeldovich and  $\text{N}_2\text{O}$  mechanisms, indicates the conclusions reached earlier in discussion of Fig. 4 for ASE40 conditions apply to the heavy-duty machines as well, that is, ignoring the  $\text{N}_2\text{O}$  route leads to an underprediction of the NO formation rate. Results predicted for the ASE40 engine, using Eqs. (4–11), are shown in Fig. 5, the format of which is similar to that in Fig. 3.

### Discussion

The results in Fig. 5 are not too different from those in Fig. 3, and little or no improvement is seen. The slope and y intercept are further from unity and zero, respectively, but the correlation coefficient and standard deviation both indicate a somewhat more linear fit. Thus, using an average value of effectiveness with the new model, including  $\text{N}_2\text{O}$  chemistry does not remove the observed trend that effectiveness increases with engine load, at least for the ASE40 engine that operates in a lower pressure range (recall that effectiveness equal to 62.8% is based on a combustion pressure of 13 atm). If effectiveness were a monotonic function of pressure, then all ASE40 data would fall below the least-squares-fit line in Fig. 5.

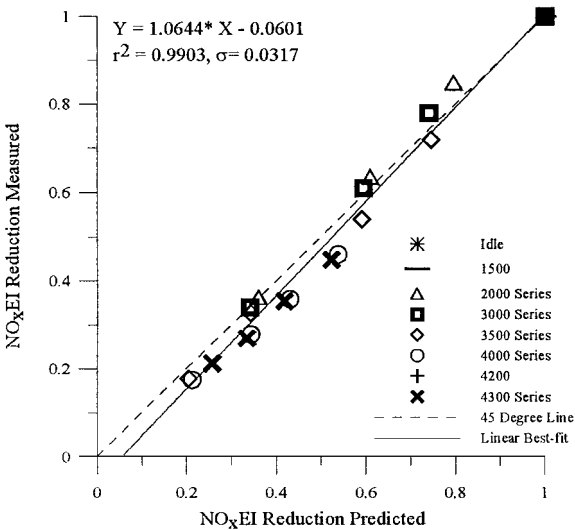


**Fig. 5** Measured vs predicted  $\text{NO}_x$  reductions for the AlliedSignal ASE40 industrial gas turbine operating over its load range either dry or with liquid water injection; the predictions are based on the new model that accounts for the lowering of stoichiometric flame temperature by water evaporation/dilution, with 62.8% effectiveness [see Eq. (11)] and corresponding decrease in NO formation rates by both the Zeldovich and nitrous oxide mechanisms.

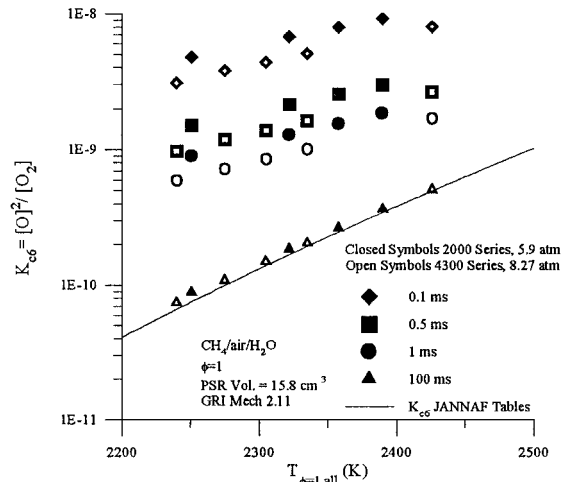


**Fig. 6** Kinetic and equilibrium calculations for O-atom concentration squared divided by  $\text{O}_2$  concentration for the ASE40 2000 and 4300 series test conditions at nominally 5.9 and 8.27 atm, respectively; methane/air/water perfectly stirred reactor residence times of 0.1, 0.5, 1.0, and 100 ms were used for the kinetic computations (symbols), and the solid line represents the equilibrium results.

For the calculations in Fig. 5 the effective third-body concentration [Eq. (8)] is evaluated at the theoretical maximum reduced stoichiometric flame temperature  $T_{\phi=1, \text{all}}$ . Using the temperature defined in Eq. (11) instead will not improve the results shown in Fig. 5 because  $[M]$  is inversely proportional to temperature [Eq. (8)]. Thus, utilizing the effective value of the inert injection temperature would lead to a lower value of  $[M]$  and decrease  $k_{5f}$  relative to  $k_{1f}$ .

An important assumption used in the model development is that O-atom equilibrium applies in the flow regions where NO forms by both the  $\text{N}_2\text{O}$  and Zeldovich mechanisms [see Eq. (5)]. Because it is generally agreed<sup>15</sup> that the former pathway is more important in the flame zone than in the burned gases, the consequences of this assumption must be evaluated.

The findings are presented in Fig. 6, the equilibrium constant based on concentrations vs  $T_{\phi=1, \text{all}}$ . Kinetic O-atom and  $\text{O}_2$  concentrations for residence times of 0.1, 0.5, 1.0, and 100 ms are used to form  $K_{c6}$  for  $\text{O}_2 \rightleftharpoons 2\text{O}$  for the ASE40 data in the 2000 and 4300 series. The symbols represent results from perfectly stirred reactor calculations with GRI Mechanism 2.11 (see Ref. 10). The solid line is based on equilibrium values from STANJAN. For each value of  $T_{\phi=1, \text{all}}$  corresponding to the engine tests, the corresponding mixture of  $\text{CH}_4$ , air, and  $\text{H}_2\text{O}$  at  $p_{s3}$  and  $T_{\phi=1, \text{all}}$  was allowed to react adiabatically for the indicated residence time. As water-to-fuel ratio is increased from zero,  $T_{\phi=1, \text{all}}$  decreases, and for any constant value of residence time  $K_{c6}$  also decreases.

The following observations are suggested by the results in Fig. 6. First, as the combustor pressure is increased (closed to open symbols), the O-atom overshoot (with respect to the equilibrium value) at a given reactor residence time decreases. This result is expected based on consideration of atom recombination rates increasing with pressure. Second, for a residence time of 100 ms (triangles), the kinetic calculations agree with the equilibrium values (solid line), as must be true for sufficiently long residence times. Finally, at a given load (2000 or 4300 series) and reactor residence time, as the water-to-fuel ratio is increased and temperature decreases, the O-atom overshoot increases relative to equilibrium because recombination rates decrease as reaction temperature is decreased.

Because the expected change in combustor residence time with water-to-fuel ratio is negligible, this last finding suggests that the contribution of the  $\text{N}_2\text{O}$  mechanism (for which the flame-front O-atom is important) increases in significance compared to the Zeldovich mechanism (for which postflame equilibrium estimates of O-atom are more appropriate) as water-to-fuel ratio is increased. Furthermore, because the magnitude of O-atom overshoot decreases as combustor pressure, that is, load, increases, the results in Fig. 6

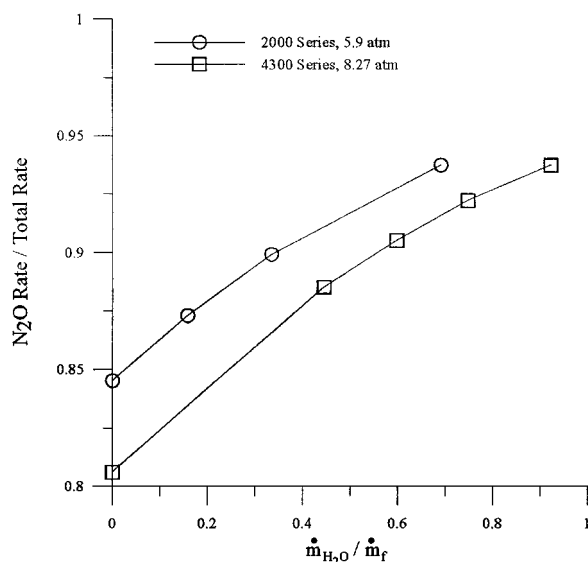


**Fig. 7 Modeled fractional contribution of the  $N_2O$  mechanism to total NO formation via both Zeldovich and  $N_2O$  routes for water-to-fuel ratios by mass used in the ASE40 2000 and 4300 series test conditions, at nominally 5.9 and 8.27 atm, respectively.**

indicate that the actual effectiveness of water injection will increase with increasing load due to less NO formation through the nitrous oxide mechanism.

In Fig. 7 the estimated fraction of total NO formation rate due to the nitrous oxide mechanism is graphed vs water-to-fuel ratio by mass for the ASE40 2000 series at approximately 5.9 atm and 4300 series at nominally 8.27 atm. The fraction was computed from the results shown in Fig. 6 as follows:

$$\frac{N_2O \text{ Rate}}{\text{Total Rate}} = \frac{k_{5f}[O]_{0.1 \text{ ms}}}{k_{1f}[O]_{100 \text{ ms}} + k_{5f}[O]_{0.1 \text{ ms}}} \quad (12)$$

where brackets with subscripts indicate O-atom concentrations at the indicated perfectly stirred reactor residence time. Specific reaction rate coefficients for Eq. (12) and Fig. 7 are evaluated at the values of  $T_{\phi=1, \text{all}}$  shown on the x axis in Fig. 6 corresponding to the various engine test points. The intent is to use the 0.1-ms value of O-atom concentration to approximate flame-front NO formation through the nitrous oxide pathway and the 100-ms value the post-flame contribution from the Zeldovich mechanism. Although this approach is simplistic, it does confirm the trend discussed in conjunction with Fig. 6 that higher pressures at higher loads (squares vs circles) suppress that portion of NO formation from the  $N_2O$  pathway at a given water-to-fuel ratio by mass.

Thus, at any given combustor power level, the primary effect of inert injection is thermal, the result of diluent phase change and subsequent dilution of the stoichiometric mixture lowering the flame temperature and slowing NO formation kinetics by both Zeldovich and nitrous oxide routes, as indicated in Fig. 4. However, the latter mechanism is associated with early times in the combustion process where the overshoot of free radicals is important. Estimates of kinetic values of O-atom in the flame zone show a small but contrary effect: Higher pressures at higher combustor loads diminish the contribution from the nitrous oxide mechanism because O-atom overshoots are smaller, and the augmentation of the Zeldovich chemistry by the  $N_2O$  reactions is less (Fig. 7).

The models utilized here demonstrate that the average effectiveness of inert injection is equal to 60–70%, depending on what NO formation chemistry is considered. As discussed by Newbury and Mellor,<sup>3</sup> this result is a consequence of the impossibility of injecting water/steam solely into the stoichiometric, NO-forming eddies in the primary zone of a conventional combustor. The other obvious candidates to explain this result are physical processes involving water injection and finite rate evaporation or mixing of diluent with the fuel and air, that is, in terms of the model, more inert reaching stoichiometric eddies as combustion pressure and temperature are

increased. Touchton<sup>1</sup> provides convincing evidence that neither is responsible for nonunity values of effectiveness.

## Conclusions

Two models for  $NO_x$  emissions reductions resulting from inert injection successfully predict those measured with water injection in the AlliedSignal ASE40 3.25-MW industrial gas turbine fired on natural gas. The empirical constant, average effectiveness, required for quantitative predictions is obtained by calibration of both models with water and steam injection data for considerably larger 150-MW heavy-duty combustion turbines burning either gas or oil. Both models are strictly thermal; that is, NO formation rates are lowered by stoichiometric flame temperature reduction as a result of evaporation of the liquid and dilution of the flame and burned gases by steam.

The first model, published previously, includes only Zeldovich NO formation kinetics, whereas the second model is based on both Zeldovich and  $N_2O$  pathways for NO formation. The lower average effectiveness found for the second model confirms that the  $N_2O$  mechanism makes a nonnegligible contribution to the emissions for operating conditions typical of all three engines considered. Neither model using equilibrium estimates of O-atom concentration correlates the empirical observation that effectiveness is enhanced somewhat over that resulting solely from dilution as engine load is increased. Kinetic calculations of O-atom, in conjunction with the flame-front formation of NO via the  $N_2O$  route, suggest that the second-order improvement in effectiveness with load results from less flame-front formation of NO through this route as combustor pressure is increased.

Comparisons with the industrial engine data indicate that either model, with appropriate value of average effectiveness, can be used for accurate predictions of the best  $NO_x$  reduction with water or steam injection. Although this conclusion is based on measurements made when burning natural gas, the results published previously showed good correlation of  $NO_x$  reductions for cases of gas and oil firing. As such, the predictions provide a benchmark against which various inert injection arrangements can be evaluated. However, the second-order effect of load on effectiveness, here suggested due to  $N_2O$  chemistry, can not be modeled with an equilibrium estimate of O-atom for combustor pressures considered here. The new model may prove more accurate than the previous model as machines with increased compressor pressure ratio appear on the market, as suggested by Fig. 4, but it is considerably more difficult to implement and would only provide a new correlation. Therefore, the conclusion of the work is that the previous technique, here used for predictions of  $NO_x$  reductions for the first time, is recommended, at least for cycles with pressure ratios less than 15.

## Acknowledgments

G. D. Myers of AlliedSignal Engines provided the ASE40 data analyzed here, and W. L. Easley, J. P. Mello, D. M. Mosbacher, M. A. Psota, and A. A. Stowe of Vanderbilt University assisted with some of the computations. J. Sanborn, P. Kawamura, and L. Hernandez of AlliedSignal Engines and J. P. Mello, now at Arthur D. Little, Inc., read an early version of the manuscript and suggested important clarifications.

## References

- Touchton, G. L., "Influence of Gas Turbine Combustor Design and Operating Parameters on Effectiveness of  $NO_x$  Suppression by Injected Steam or Water," *Journal of Engineering for Gas Turbines and Power*, Vol. 107, Oct. 1985, pp. 706–713.
- Liever, P. A., Smith, C. E., Myers, G. D., Hernandez, L., and Griffith, T., "CFD Assessment of a Wet, Low- $NO_x$  Combustion System for a 3MW-Class Industrial Gas Turbine," American Society of Mechanical Engineers, Paper 98-GT-292, June 1998.
- Newbury, D. M., and Mellor, A. M., "Semiempirical Correlations of  $NO_x$  Emissions from Utility Combustion Turbines with Inert Injection," *Journal of Propulsion and Power*, Vol. 12, No. 3, 1996, pp. 527–533.
- Toof, J. L., "A Model for the Prediction of Thermal, Prompt, and Fuel  $NO_x$  Emissions from Combustion Turbines," *Journal of Engineering for Gas Turbines and Power*, Vol. 108, April 1986, pp. 340–347.

<sup>5</sup>Malte, P. C., and Pratt, D. T., "The Role of Energy-Releasing Kinetics in NO<sub>x</sub> Formation: Fuel Lean, Jet Stirred CO–Air Combustion," *Combustion Science and Technology*, Vol. 5, Nos. 5 and 6, 1974, pp. 221–231.

<sup>6</sup>Nicol, D. G., Malte, P. C., and Steele, R. C., "Simplified Models for NO<sub>x</sub> Production Rates in Lean-Premixed Combustion," American Society of Mechanical Engineers, Paper 94-GT-432, June 1994.

<sup>7</sup>Reynolds, W. C., "STANJAN Version 3.93," Dept. of Mechanical Engineering, Stanford Univ., Stanford, CA, 1987.

<sup>8</sup>Polifke, W., Döbbeling, K., Sattelmayer, T., Nicol, D. G., and Malte, P. C., "A NO<sub>x</sub> Prediction Scheme for Lean-Premixed Gas Turbine Combustion Based on Detailed Chemical Kinetics," American Society of Mechanical Engineers, Paper 95-GT-108, June 1995.

<sup>9</sup>Easley, W. L., Mellor, A. M., and Plee, S. L., "NO Formation and Decomposition Models for DI Diesel Engines," Society of Automotive Engineers, Paper 2000-01-0582, March 2000.

<sup>10</sup>Bowman, C. T., Hanson, R. K., Davidson, D. F., Gardiner, W. C., Lissianski, V., Smith, G. P., Golden, D. M., Frenklach, M., and Goldenberg, M., URL:[http://www.me.berkeley.edu/gri\\_mech/](http://www.me.berkeley.edu/gri_mech/) [cited 15 Sept. 1997].

<sup>11</sup>Mello, J. P., and Mellor, A. M., "Modeling NO<sub>x</sub> Emissions from Lean-Premixed Turbine Combustors with Swirling, Nonuniform Fuel/Air Mixtures," AIAA Paper 99-2773, July 1999.

<sup>12</sup>Mellor, A. M., Mello, J. P., Duffy, K. P., Easley, W. L., and Faulkner, J. C., "Skeletal Mechanism for NO<sub>x</sub> Chemistry in Diesel Engines," Society of Automotive Engineers, Paper 981450, May 1998; also *SAE 1998 Transactions and Journal of Fuels and Lubricants*, Vol. 107, No. 4, 1999, pp. 786–801.

<sup>13</sup>Troe, J., "Thermal Dissociation and Recombination of Polyatomic Molecules," *Proceedings of the Fifteenth Symposium (International) on Combustion*, The Combustion Institute, Pittsburgh, PA, 1974, pp. 667–680.

<sup>14</sup>Mello, J. P., and Mellor, A. M., "NO<sub>x</sub> Emissions from Direct Injection Diesel Engines with Water/Steam Dilution," Society of Automotive Engineers, Paper 1999-01-0836, March 1999.

<sup>15</sup>Magruder, T. D., McDonald, J. P., Mellor, A. M., Tonouchi, J., Nicol, D. G., and Malte, P. C., "Engineering Analysis for Lean Premixed Combustor Design," AIAA Paper 95-3136, July 1995.